Analytical study for the comparison between hygroscopic and Rankine cycle. An exergy approach

Malena Potesta González [a], Roberto Martínez-Pérez [a], Andrés Meana-Fernández [a], Francisco J. Rubio-Serrano [b], Antonio J. Gutiérrez-Trashorras [a,*]

[a] *Energy Department, Polytechnic School of Engineering, Universidad of Oviedo, 33203, Energy Building, Campus of Viesques, Gijón, Asturias, Spain*
[b] *IMATECH, IMASA Technologies, S.L.U. St, Carpinteros 12, 28670 Villaviciosa de Odón, Madrid, Spain*

ARTICLE INFO

ABSTRACT

The Hygroscopic Cycle Technology (HCT) is a proprietary technology that allows producing energy with better performance and more sustainable than traditional Rankine Cycle (RC). The aim of this study is to implement analytical models for comparing the performance of HCT and RC operating at industrial scale conditions. The study focuses on energy and exergy analysis in order to compare the cycles and determine the equipment with the higher irreversibilities for providing a base to improve them. A base case of each cycle has been defined and compared. Also, a sensitivity analysis of the main parameters of the cycles has been done. Grassman diagrams of the base cases have been studied to quantify the exergy distribution and destruction. According to the results obtained exergy efficiency of the HCT can be 2.52% greater than that of the regenerative RC for high cooling temperatures. For cooling, dry coolers can be used with ambient temperatures of up to 46 °C for HCT while for the RC it is limited to 38 °C. The variables with the greatest influence on the exergy efficiency are the condensing pressure and the boiler air–fuel ratio. In the HCT, due to the excess of air required for complete combustion, the exergy destruction rate in the boiler can be increased by 1% and the exergy efficiency of the HCT can be 1.3% lower than the value for the stoichiometric air–fuel ratio. For a 10 MW power plant the exergy of the fuel in absolute terms was lower for the HCT (37.08 MW) than for the RC (37.92 MW).

1. Introduction

The current global energy crisis [1] has highlighted the need for increased efforts to use more efficient and sustainable energy production systems. The actual trend is to depend less on non-renewable energies and more on renewable sources to reduce CO_2 emissions when producing electricity and heat [2]. Electricity is typically produced by thermoelectrical power plants (through a renewable or non-renewable sources) using mainly a Rankine Cycle (RC) [3]. In 2021, over 71 % of the energy was supplied in thermoelectrical power plants [2]. Since RC is of great importance in energy production, methods of improving its performance have been widely studied over the years, proposing different solutions widely known [4]. Typical methods are supercritical, reheated, regenerative and binary vapor cycles. These improvements aim to increase the cycle's efficiency by increasing the operating pressure of the boiler, which raises the temperature at which the heat absorption takes place in the boiler; and/or decreasing the operating

pressure of the condenser, and thus the temperature at which heat is rejected [5]. Instead of varying conditions of the RC it is also possible to improve its performance using different working fluids. The Organic Rankine Cycle (ORC) works with a great variety of organic fluids and has proved to be an efficient alternative to RC at low-grade power production [6]. Since the latent heat of vaporization of organic fluids is lower than that of water the ORC can work with low-grade temperature heat sources [7]. However, ORC performance is strongly conditioned by heat source characteristics and system design [8] and, also, by the type of organic fluids used [9]. Not only organic fluids are suitable for the ORC but also zeotropic mixtures. Xu et al. [10] pointed out that the exergy efficiency of ORC using zeotropic mixtures is higher than with pure fluids. Tian et al. [11] carried out an exergy analysis of a parallel two-stage ORC driven by waste heat from LNG-fueled ship using zeotropic mixtures. They concluded that maximum exergy efficiency was 23.28%. Kalina Cycle (KC) is another RC variation that uses ammonia water as a working fluid. It is also conceived to work with low-medium temperature heat sources and can display higher performance than RC and basic

---

Nomenclature

$\dot{B}$	Exergy rate
b	specific exergy
c	velocity
c_p	specific heat capacity
c_p^{ε}	mean molar isobaric exergy capacity
F	air–fuel ratio
g	gravity
h	specific enthalpy
H	enthalpy
$\dot{m}$	Mass flow rate
$\dot{n}$	mols per unit time
P	pressure
$\dot{Q}$	thermal power
R	ideal gas constant
s	specific entropy
T	temperature
$\dot{W}$	mechanical power
w	specific work
x	molar fraction
z	elevation

Greek symbols

β	experimental biomass coefficient
Δ	difference
ε	relative error
η	efficiency
ϕ	exergy destruction ratio

Subscripts

0	dead state
air	air
b	boiler
bd	bleeding
c	condensing
ch	chemical
cr	cooling reflux
d	destruction
dc	dry coolers
ex	exergy
f	fuel
fl	flame
fumes	fumes
gases	gases
i	stream

in	inlet
j	component
k	thermal reservoir
max	maximum
net	net
out	outlet
P	products
pu	pump
p	purges
ph	physical
R	reactants
re	relative
r	cooling
real	real
s	isentropic
st	stoichiometric
t	thermal
tu	turbine
total	total
u	useful
v	vapor

Superscripts

0	standard

Acronyms

CV	Control Volume
EES	Engineering Equation Solver
GC	Goswami Cycle
KC	Kalina Cycle
ORC	Organic Rankine Cycle
RC	Rankine Cycle

Chemical symbols

$[Cl]^-$	chloride ions
$[F]^-$	fluoride ions
$[Na]^+$	sodium ions
$[NH_4]^+$	ammonium
$[NO_2]^-$	nitrites
$[NO_3]^-$	nitrates
$CaCO_3$	calcium carbonate
CO_2	carbon dioxide
H_2O	water
N_2	nitrogen
O_2	oxygen

ORC [12]. Merger et al. [13] showed that KC exergy efficiency can be 25% higher than that of an ORC using R245fa. However, when the ORC uses n-Pentane as a working fluid its thermal and exergy efficiencies are better than those of the KC [14]. The Goswami Cycle (GC) is, also, a relatively new cycle that operates with low-grade and mid-grade temperature heat sources [15]. This cycle presents a combination of an ammonia–water vapor absorption cycle and an ammonia-based ORC for cooling and mechanical power [16]. Fontalvo et al. [17] carried out an exergy analysis of the GC and concluded that devices with great exergy destruction were the absorber, the boiler and the turbine. A new combination of a KC and a GC was presented in [18] along with a new exergy optimization procedure. Results showed that for given operational parameters maximum exergy efficiency achieved was 18.79%. Even though these variants of the RC improve performance they have to face other two problems that come along with the RC: condensing water at high ambient temperature and water consumption. As expressed in [19]

the ORC is affected by the fluctuation of ambient temperature. Moreover, locations with tropical climates are not suitable for thermal cycle implementation [20]. Regarding water consumption, the average water footprint of electricity and heat production was rated as 4241 m³/TJ [21]. The high needs for cooling water poses a serious problem in areas with water scarcity [22].

The Hygroscopic Cycle Technology (HCT) [23] is a proprietary technology that asses the abovementioned problems related to thermal cycles. The HCT was developed by F. Rubio-Serrano et al. [24] and has been in the state of art since 2010 as "RC with absorption stage using hygroscopic compounds". The layout of the HCT (Fig. 1) is similar to that of the RC. The main difference is that the condenser of the RC is replaced by a mixing chamber (absorber) in the HCT [25]. Condensation is produced by absorption in using the properties of the salts dissolved in water as hygroscopic compounds. It allows condensing and refrigerating the cycle at higher temperatures than in Rankine cycle, making it
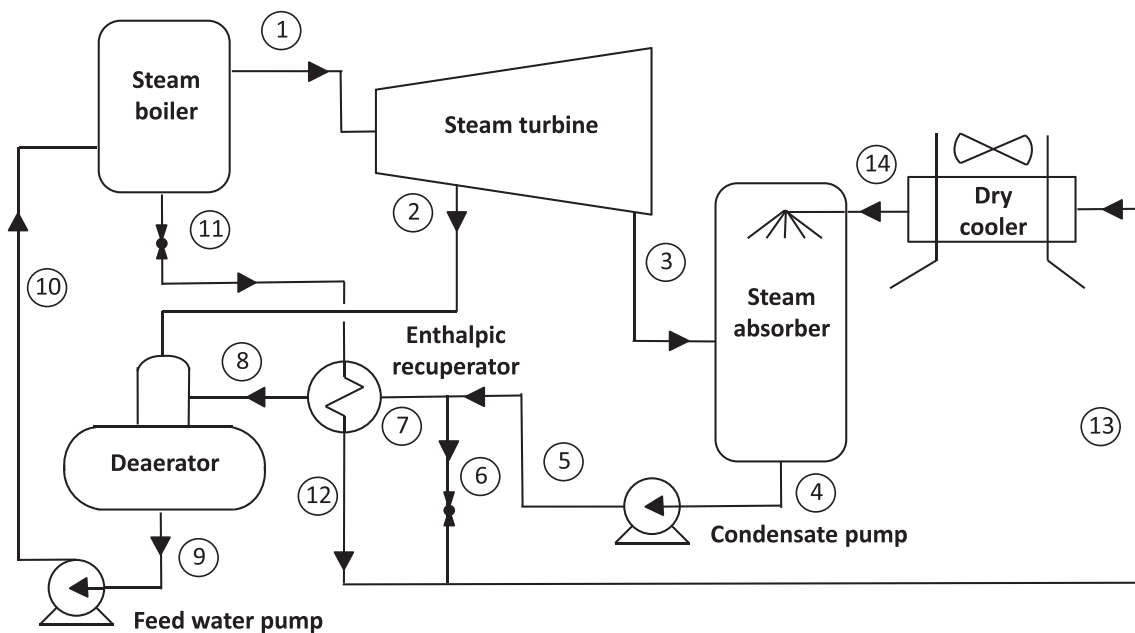
Fig. 1. Scheme of the Hygroscopic Cycle Technology.

possible to refrigerate by dry coolers and avoiding the water consumption for cooling. Desorption of hygroscopic compounds takes place in the boiler drum. The hygroscopic compounds remain in the saturated liquid at the bottom of the drum. Consequently, the purge stream contains most of the hygroscopic compounds. A small part of the hygroscopic compounds is carried away by the steam leaving the boiler, so it is very important to control the concentration of these compounds in the steam leaving the boiler in order to comply with the requirements specified by the turbine manufacturer and to avoid corrosion, scaling, etc. For concentration of hygroscopic compounds lower than 0.01%, like those of existing installations at industrial level, it has been experimentally corroborated that they do not pose a risk to the metallurgy of the equipment nor pipelines [26]. Consequently, safety and efficiency of the turbine are not reduced by the effect of the hygroscopic compounds with those low concentrations.

According to Fig. 1, condensation of the exhaust steam takes place in the absorber, where the steam (3) is mixed with a cooling reflux (13, 14), which contains dissolved hygroscopic compounds [27]. Those compounds are obtained from the purges stream (11) of the boiler. The energy of that stream is partially recovered in a heat exchanger (enthalpic recuperator). The use of hygroscopic compounds allows condensing temperatures to be raised above the saturation temperature of the pure water for a stated condensing pressure in the absorber [28]. The HCT presents two main advantages over the RC due to the absorption process [29]:

● The condensing pressure decreases for a given cooling temperature (state 14 in Fig. 1); therefore, the electrical efficiency of the plant is improved.
● The condensing temperature rises for a given condensing pressure; therefore, the condensation energy can be dissipated in an air cooler instead of a cooling tower. This dry mode of condensation allows saving tones of water. In fact, water saving is the one of the main benefits of HCT since water scarcity constitutes a serious problem in electricity production [30].

In addition, the HCT is not limited only to low-grade power productions as the ORC and KC. It can be implemented in different power plants such as [24]: thermoelectric plants, combined cycles, biomass power plants and nuclear power plants.

The first pilot plant of the HCT is owned by IMATECH (IMASA Technologies). It was developed by F. Rubio-Serrano et al. and located in Gijón (Spain) [31]. The HCT has been already implemented at industrial scale in biomass power plants from 12.5 MW to 25 MW, all working with low concentrations (less than 0.01%) of hygroscopic salts [25]. The first power plant to introduce the HCT at industrial scale was the 12.5-MWe biomass power plant of "Vetejar" (Spain) [24]. This power plant is owed by "Oleícola el Tejar" and located in Palenciana (Córdoba, Spain) [32]. In the first instance, cooling of the steam was produced with a cooling tower. However, due to water scarcity in the area a battery of air coolers was installed in 1997 to reduce the water consumption. An adiabatic spray was also installed to reduce the temperature of the water outside the air coolers [24]. Because of the water scarcity, the high temperature reached in the location and degradation of the air coolers due to the spray system in 2017 the HCT was finally incorporated. Main benefits of the implementation of HCT to that plant were [24]: higher annual production of electricity, increment of the availability of the power plant, lower electrical consumption of the air coolers, and the net electrical efficiency is increased by 2.5%, without cooling water consumption. According to the advantages of HCT, it is of direct application in installations that have problems of water shortage and/or high ambient temperatures. These conditions are common in the southern areas of Spain. In these areas there are many biomass plants belonging to the olive oil industry. To date, most of the facilities that have implemented HCT in their power production plants belong to this sector and are biomass plants that use olive residues as fuel. However, HCT can be applied in other types of power plants. In fact, it is already starting to be implemented in other countries and in other types of power plants [31].

Exergy, unlike energy, can be destroyed due to the irreversibilities of the systems. The principal application of exergy analysis is to quantify the inefficiencies of systems in order to design better processes or equipment with lower exergy destruction rates. As J. Moran [33] points out, exergy analysis is applied to the design and optimization of thermal and chemical systems. Exergy analysis provides more detailed and useful information of the system studied, more data on its efficiency and a better knowledge of the most inefficient parts of the system. Exergy analysis has become a vital feature for obtaining a better understanding of the processes, determine the quality of the energy used and quantify the inefficiency sources. The existing studies on the HCT focus especially on the thermodynamic analysis and on the influence of some variables.

However, in the literature there are not studies on the exergy analysis of the HCT. Consequently, it is, precisely, in the field of exergy that more research is needed, considering both the chemical and physical exergy. The aim of this research is to implement analytical models for comparing HCT and RC performance, highlight the benefits of HCT and determine the equipment with the higher irreversibilities for providing a base to improve the HCT, based on an exergy analysis and evaluating both chemical and physical exergy of the cycles. Analytical models of both RC and HCT operating at industrial scale conditions (hygroscopic compounds concentration lower than 0.01%) are developed. The boiler of the HCT is studied in detail since it is, foreseeably, the device with the higher destruction exergy rate. In addition, a comparison between the exergy efficiency of the HCT with that of the regenerative RC is presented. Exergy destruction rates of each device of both the HCT and the RC are compared to identify the devices with greater losses. Finally, sensitivity analysis of the HCT and the boiler of the HCT are addressed. EES software is used to do the abovementioned analysis.

2. Methodology

Analytical models of the HCT and the RC have been developed to perform the comparison between them, including the exergy analysis. The models have been performed according to the schemes in Fig. 1 and Fig. 2. Fig. 1 displays the scheme of the HCT and, as it was explained before, is very similar to the RC cycle. Instead of a condenser, HCT includes an open heat exchanger (a mixing chamber) in which the condensation of water by absorption takes place. The purges of the boiler are used for providing the necessary hygroscopic compounds for the absorption process. Fig. 2 shows the scheme of the traditional regenerative RC with deaerator and a bleeding at an intermediate state (2) of the turbine. In addition, the cooling circuit is presented for the heat rejection of the cycle. The main differences between the HCT and regenerative RC are that in HCT absorber replaces the condenser of the RC, a closed heat exchanger is used for recovering the energy of the purges extracted from the boiler, and the refrigeration is provided by means of a closed loop with dry coolers without cooling water.

2.1. Energy and exergy analysis

Eqs. (1) and (2) correspond to mass and energy balances at steady flow conditions respectively applied to a Control Volume (CV).

$$\sum_{in} \dot{m}_i = \sum_{out} \dot{m}_i \tag{1}$$

$$\dot{Q} - \dot{W} = \sum_{out} \dot{m}_i \left[h_i + \frac{c_i^2}{2} + g z_i \right] - \sum_{in} \dot{m}_i \left[h_i + \frac{c_i^2}{2} + g z_i \right] \tag{2}$$

Being:

$\dot{m}_i$: mass flow rate at inlets and outlets of the CV.

h_i: specific enthalpy of the fluid at inlets and outlets of the CV.

c_i: velocity of the fluid at inlets and outlets of the CV.

z_i: elevation at inlets and outlets of the CV.

$\dot{Q}$: thermal power transferred into the CV.

$\dot{W}$: mechanical power produced in the CV.

g: gravity.

Kinetic and potential energy changes can be neglected in both HCT and RC models.

Exergy balance equation is expressed in Eq. (3):

$$\sum_{in} \dot{B}_i - \sum_{out} \dot{B}_i + \sum \left(1 - \frac{T_0}{T_k} \right) \dot{Q}_k - \dot{W} - \dot{B}_d = 0 \tag{3}$$

being:

$\dot{B}_i$: exergy rate of the stream at inlets and outlets of the CV.

T_0: temperature of dead state.

$\dot{Q}_k$: heat transfer rate exchanged with a thermal reservoir.

T_k: average temperature of heat transfer exchange.

$\dot{B}_d$: rate of exergy destruction.

The terms in Eq. (3) can also be named as net stream exergy rate variation (Eq. (4)), exergy rate of heat transfer (Eq. (5)) and exergy rate of mechanical power (Eq. (6))

$$\Delta \dot{B} = \sum_{in} \dot{B}_i - \sum_{out} \dot{B}_j \tag{4}$$

$$\dot{B}_{\dot{Q}} = \sum \left(1 - \frac{T_0}{T_k} \right) \dot{Q}_k \tag{5}$$

$$\dot{B}_{\dot{W}} = \dot{W} \tag{6}$$

Physical and chemical exergy rate [34 35 36] of a stream ($\dot{B}_i$) is calculated as in Eq. (7):
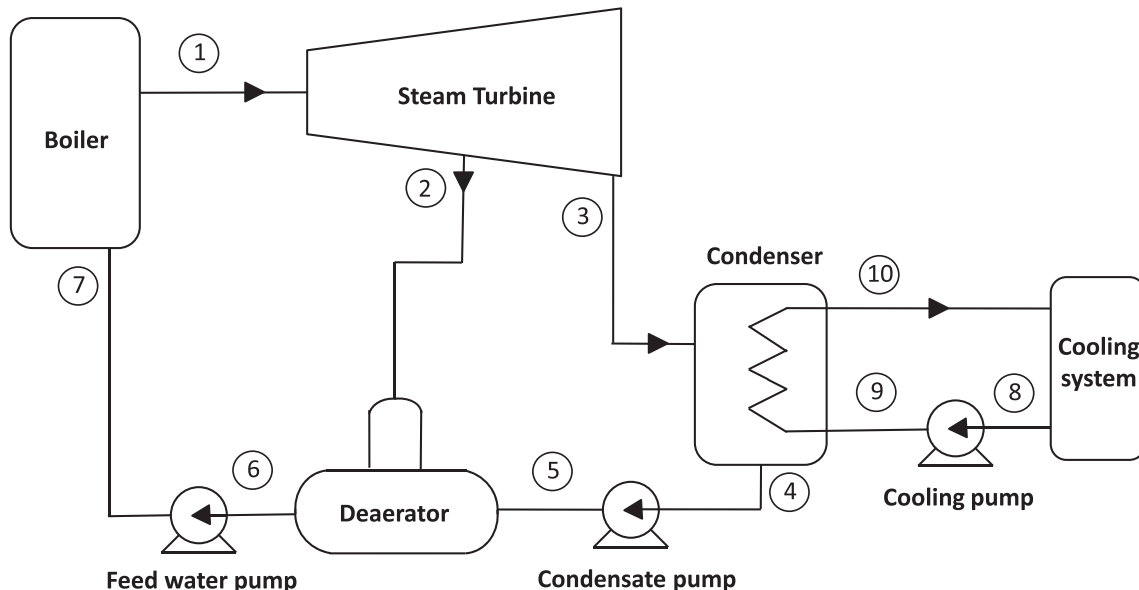

Fig. 2. Scheme of the regenerative Rankine Cycle with deaerator.

$$\dot{B}_i = \dot{B}_{ph} + \dot{B}_{ch} = \dot{m}_i[(h_i - h_0) - T_0(s_i - s_0)] + \dot{n}_i\left[\sum_j x_j b_{ch}^0 + RT_0\sum_j x_j \ln x_j\right] \tag{7}$$

h_0 and s_0 are enthalpy and entropy of the fluid at dead state ($P_0 = 1$ bar and $T_0 = 298$ K) respectively.

$\dot{n}_i$: total mols per unit time.

x_j: molar fraction of each component of the fluid.

b_{ch}^0: standard molar chemical exergy of each component of the fluid.

Exergy destruction ratio (ϕ_i) of the equipment is presented in Eq. (8). $\dot{B}_{in}$ is total exergy rate incoming the CV.

$$\phi_i = \frac{\dot{B}_{d,i}}{\dot{B}_{in}} \tag{8}$$

Isentropic efficiencies of the turbine and pumps are calculated as in Eqs. (9) and (10).

$$\eta_{s,tu} = \frac{w_{real}}{w_s} = \frac{h_{in} - h_{out}}{h_{in} - h_{out_s}} \tag{9}$$

$$\eta_{s,pu} = \frac{w_s}{w_{real}} = \frac{h_{out_s} - h_{in}}{h_{out} - h_{in}} \tag{10}$$

w_{real}: specific work of turbine or pump.

w_s: specific work of the ideal (isentropic) process.

The values of isentropic efficiencies of turbines and pumps have been considered of 85% and 77% respectively [37 38 39].

Thermal efficiency (η_t) and exergy efficiency (η_{ex}) of a cycle (Eqs. (11) and (12)) are given as:

$$\eta_t = \frac{\dot{W}_{net}}{\dot{Q}_{in}} \tag{11}$$

$$\eta_{ex} = \frac{\dot{B}_u}{\dot{B}_{in}} \tag{12}$$

The efficiency increase (ε_η) of the HCT with respect to RC is calculated according to Eq. (13)

$$\varepsilon_\eta = \frac{\eta_{HCT} - \eta_{RC}}{\eta_{RC}} \tag{13}$$

$\dot{B}_u$ represents the total useful exergy rate. Notice that for a cycle $\dot{B}_u = \dot{W}_{net}$.

For the models, Eqs. (1)–(10) have been particularized to the operating conditions of the devices involved in the HCT and regenerative RC. The model of the HCT (Fig. 1) has been developed for dissolutions with very low concentrations of hygroscopic compounds. Those compounds are the proper salts contained in water (with concentrations lower than 0.01%) that are the ones used in actual HCT at industrial scale and the values of the properties for the dissolution can be approximated by those of pure water.

Since the HCT has so far been mainly implemented in biomass power plants, and specifically in the olive oil industry, the fuel selected in this study for the boiler of both the HCT and RC models is alperujo or orujillo, a type of biomass obtained from olives. Fig. 3 a) and Fig. 3 b) show the scheme of the boiler for HCT and RC respectively. The design difference is that the purges are continuously extracted giving rise to the purge stream in the case of HCT.

Adiabatic combustion is simulated to calculate the adiabatic flame temperature. Once the combustion reaction is adjusted, the adiabatic flame temperature can be obtained following an iterative method. Enthalpies of reactants and products of the combustion are equated, and adiabatic flame temperature is calculated (Eq. (14))

$$H_R = H_P \tag{14}$$

H_R: enthalpy of the reactants.

H_P: enthalpy of the products.

The specific exergy of fuel can be calculated with Szargut and Styrylska's correlation [40] (Eq. (15))

$$b_{ch} = \beta \bullet LHV \tag{15}$$

LHV: lower heating value of the fuel. Since the fuel used is orujillo LHV is estimated to be 18246.42 kJ/kg [41].

β (Eq. (16)) is an experimental coefficient only valid when $0.5 < \frac{O}{C} \leq 2$

$$\beta = \frac{1.0414 + 0.0177\left(\frac{H}{C}\right) - 0.3328\left(\frac{O}{C}\right)\left[1 + 0.0537\left(\frac{H}{C}\right)\right]}{1 - 0.4021\left(\frac{O}{C}\right)} \tag{16}$$

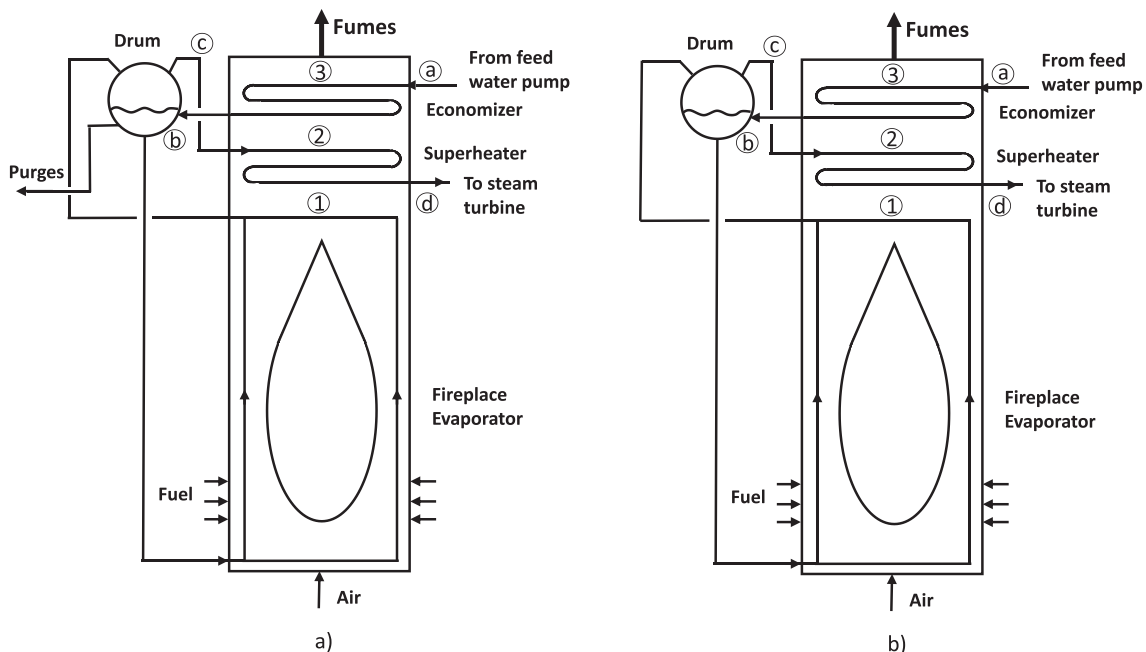O: moles of oxygen in the biomass.

C: moles of carbon in the biomass.

Fig. 3. A) boiler of the hct b) boiler of the rc.

H: moles of hydrogen in the biomass.

The values for orujillo are $\frac{O}{C} = 0.6$, $\frac{H}{C} = 1.4$[34], and $\beta = 1.121$.

Exergy rate of the fuel is finally calculated multiplying mass flow of fuel and specific exergy (Eq. (17)):

$$\dot{B}_{in} = \dot{m}_f \bullet b_{ch} \qquad (17)$$

$\dot{m}_f$: mass flow rate of fuel.

Exergy rate of combustion gases (Eq. (18)) is divided in chemical exergy (Eq. (19)) and physical exergy (Eq. (20)). Both can be obtained from Eqs. (19)–(21) [36].

$$\dot{B}_{gases} = \dot{B}_{ch} + \dot{B}_{ph} = \dot{n}_{P,total}b^0_{P,ch} + \sum_i \dot{n}_i b_{ph,i} \qquad (18)$$

$$b^0_{P,ch} = \sum_i x_i b^0_{ch} + RT_0 \sum_i x_i lnx_i \qquad (19)$$

$$\sum_i \dot{n}_i b_{ph,i} = (T - T_0)\sum_i \dot{n}_i c^\varepsilon_{p,i} + \dot{n}_{P,total}Rln\left(\frac{P}{P_0}\right) \qquad (20)$$

$\dot{n}_{P,total}$: total moles per unit time of combustion gases.

$\dot{n}_i$: moles per unit time of each component of combustion gases (CO_2, H_2O, N_2 and O_2).

x_i: molar fraction of each component of combustion gases.

b^0_{ch}: standard molar chemical exergy of combustion gases.

In the case of study outlet pressure of gases, P, is equal to P_0, therefore second term of Eq. (20) is null.

$c^\varepsilon_{p,i}$ is mean molar isobaric exergy capacity at constant pressure [36], estimated in Eq. (21) using the specific heat capacity at constant pressure (c_p), that can be expressed as a polynomic function of temperature with tabulated coefficients for each gas.

$$c^\varepsilon_{p,i} = \frac{1}{T - T_0}\left[\int_{T_0}^T c_p dT - T_0 \int_{T_0}^T \frac{c_p dT}{T}\right] \qquad (21)$$

T: temperature of the gases.

Exergy of combustion gases is evaluated at adiabatic flame temperature and fumes outlet temperature.

A vital parameter for the performance of boilers is the air–fuel ratio. In order to quantify the excess of air, relative air–fuel ratio (F_{re}) is defined. It is calculated as the air–fuel ratio (F) divided by the stoichiometric air–fuel ratio (F_{st}) (Eq. (22)).

$$F_{re} = \frac{F}{F_{st}} \qquad (22)$$

Data from Sartor et al. [42] were used to validate the model with respect to the air–fuel ratio of the boiler. The model has been applied to the biomass used by those authors in their research to compare the adiabatic flame temperature obtained for dry biomass, 10% and 20% humidity of the biomass at different values of F_{re}. The values of excess of air in this type of boilers, according to [43], reach values of the order of 20%, so the values studied in this work belong to the interval $1 \leq F_{re} \leq 1.2$.

Thermal efficiency ($\eta_{t,b}$) and exergy efficiency ($\eta_{ex,b}$) of the boiler (Eqs. (23) and (24)) are given as:

$$\eta_{t,b} = \frac{\dot{Q}_{in}}{\dot{m}_f \bullet LHV} \qquad (23)$$

$$\eta_{ex,b} = 1 - \frac{\dot{B}_{d,b} + \dot{B}_{fumes}}{\dot{B}_{in}} \qquad (24)$$

where $\dot{B}_{d,b}$ is the exergy destruction rate of the boiler and $\dot{B}_{fumes}$ is the exergy rate of the fumes.

For the analytical model of the cycles, the EES software [44] has been chosen mainly because of its extensive thermodynamic database and for all the analysis possibilities that it offers (graphs, parametric analysis,

implementation of functions, etc.). The software allows the user to enter the equations and starting data of the system, call the functions and calculate all variables. At the same time, it offers the possibility of presenting the values of all variables in an array table and to include a process diagram window, in which the input and output variables can be displayed.

2.2. Experimental contrast

For the validation of the models developed and before elaborating the exergy analysis, the data analytically obtained must be contrasted with the experimental data. For this purpose, a contrast is carried out at pilot scale, taking as a reference the experimental data extracted from the pilot plant of the HCT previously mentioned. The pilot plant [29] is a reduced scale model of the Hygroscopic Cycle. It has a 100 kW$_t$ gas fire-tube boiler, with a maximum steam production capacity of 110 kg/h at 14 bar and 200 °C. The difference with a real plant is that, instead of a turbine there is a throttling valve. This valve makes it possible to simulate the operating conditions of a steam turbine in terms of pressures, temperatures and flow rates at the inlet and outlet of the turbine by means of a supervisory control and data acquisition (SCADA) system. The expansion in the valve is recorded in a PLC and the data is displayed in the SCADA, which calculates the theoretical electrical power that would be produced by the equivalent turbine. The scale of the plant allows producing over 30 kW of power production. For the validation of the RC, a shell and tube condenser was used instead of the absorber.

Uncertainty and error analysis of the pilot plant.

In the test plant, flowmeters with accuracy ± 0.5% were located in the pipelines to measure the all the mass flow rates. Pressure sensors Aplisens PCE-28, with accuracy ± 0.5% were utilized to measure the pressures at inlets and outlets of the equipment. Several cooper-constantan thermocouples T-type, with uncertainty ± 0.2 °C were utilized to measure temperatures at inlets and outlets of the equipment. Also, platinum resistances Pt100, with accuracy ± 0.1 °C were used to measure the temperatures at the inlets and outlets of the absorber to obtain more accurate data. Purges in all streams were used for taking samples of the fluid. Data acquisition equipment with an accuracy of 0.004% was used.

The absolute errors of the calculated powers were obtained by error analysis of the equations used. For the thermal power exchanged between the fluid and the sources or sink in steady flow and according to First Low of Thermodynamics (Eq. (25)):

$$\dot{Q} = \sum_{out} \dot{m}_i h_i - \sum_{in} \dot{m}_i h_i \qquad (25)$$

Appling the error theory (Eq. (26)):

$$\Delta\dot{Q} = \sum_{out}\left|\frac{\partial\dot{Q}}{\partial\dot{m}_i}\right|\Delta\dot{m}_i + \sum_{out}\left|\frac{\partial\dot{Q}}{\partial h_i}\right|\Delta h_i + \sum_{in}\left|\frac{\partial\dot{Q}}{\partial\dot{m}_i}\right|\Delta\dot{m}_i + \sum_{in}\left|\frac{\partial\dot{Q}}{\partial h_i}\right|\Delta h_i \qquad (26)$$

Consequently, the absolute error in calculated thermal powers is given by Eq. (27):

$$\Delta\dot{Q} = \sum_{out}h_i\Delta\dot{m}_i + \sum_{out}\dot{m}_i\Delta h_i + \sum_{in}h_i\Delta\dot{m}_i + \sum_{in}\dot{m}_i\Delta h_i \qquad (27)$$

Analogously, for calculated mechanical powers, the absolute error is obtained by Eq. (28):

$$\Delta\dot{W} = \sum_{in}h_i\Delta\dot{m}_i + \sum_{in}\dot{m}_i\Delta h_i + \sum_{out}h_i\Delta\dot{m}_i + \sum_{out}\dot{m}_i\Delta h_i \qquad (28)$$

Relative error for both thermal and mechanical powers are obtained by Eq. (29) y Eq. (30), respectively.

$$\varepsilon_{\dot{Q}} = \frac{\Delta\dot{Q}}{\dot{Q}} \qquad (29)$$

$$\varepsilon_{\dot{W}} = \frac{\Delta \dot{W}}{\dot{W}} \tag{30}$$

2.3. Simulations

Once the models have been developed and experimentally contrasted, a power production of 10 MW has been proposed to study and obtain conclusions on the application and advantages of the hygroscopic cycle with more suitable values on an industrial scale. For the comparison between RC and HCT, a base case has been defined. For that base case, net power production is fixed at 10 MW and the air–fuel ratio (F) is set to be the stochiometric ratio ($F_{st} = 5.31$ kg air/kg fuel). A cooling temperature of 31 °C is also fixed in both cycles. That temperature is achieved with a pressure at the absorber of 0.0865 bar for the HCT and a condensing pressure of 0.1298 bar for the RC. The ambient temperature is set to be 25 °C. At this temperature, the RC cooling system can also work with dry coolers. Pressure and temperature at the boiler are also fixed in both cycles at 90 bar and 500 °C. In addition, the pressure of the bleeding (P_{bd}) is maintained at 3 bar, the temperature difference between the inlet and outlet of the dry coolers (ΔT_{dc}) is 12 °C and the temperature of the fumes is 160 °C for both cycles. The condensate at the exit of the RC condenser is subcooled by 3 °C and the Approach of that condenser is 5 °C.

In order to make the cycles comparable, and given the same ambient temperature, the cooling temperature in both cycles must be identical for them to operate under the same conditions in each case studied. The minimum difference between these temperatures is set at 6 °C to ensure the correct operation of the dry coolers. For the base case, the ambient temperature is 25 °C, so the cooling temperature (T_r) is set at the minimum possible, which is 31 °C. The temperature difference between the inlet and outlet of the dry coolers (ΔT_{dc}) is fixed at 12 °C. According to the design of the HCT, the temperature at the inlet of the dry coolers is approximately the condensing temperature, so the difference between the cooling and condensing temperatures is 12 °C, and the condensing temperature (T_c) is 43 °C. At this temperature the condensing pressure (P_c) is 0.0865 bar. In the case of the RC, the temperature difference between the inlet and outlet of the dry coolers is also fixed at 12 °C, so if the cooling temperature is 31 °C, the fluid temperature at the inlet of the dry coolers is 43 °C. Taking into account the value of the condenser approach parameter (5 °C), the temperature of the condensate at the condenser outlet is 48 °C. It is subcooled by 3 °C, so the condensing temperature is 51 °C. At this temperature, the condensing pressure is 0.1298 bar. The same calculation procedure is used to compare the two cycles at other cooling temperatures. Consequently, the condensing pressure of the RC is greater than that of the HCT for the same cooling temperature.

Cycles are compared for the base case and a sensitivity analysis of condensing pressure, energy and exergy efficiencies of the cycles is performed varying the cooling temperature but setting it to be equal in both cycles in order to make them comparable.

Once the comparison is done, several sensitivity analyses are carried out for the HCT. The sensitivity analyses study the influence of the condensing pressure in thermal and exergy efficiencies and the cooling temperature. For the boiler, the sensitivity analyses examine the influence if the air–fuel ratio in the exergy destruction rate and the exergy efficiency of the HCT.

3. Results and discussion

3.1. Experimental contrast

HCT and RC models were validated using the experimental data from the pilot plant. Data from the models and the pilot plant were compared with condensing pressure (P_c) ranging between 0.03 bar and 0.15 bar, and boiler pressures (P_b) from 5 to 11 bar. Also, different mass flow rates

of vapor ($\dot{m}_v$) at the outlet of the boiler were used for the test according to Fig. 4. Values of the steam temperature at the inlet of the condenser/absorber (T_v) versus the condensing pressure for different pressures in the boiler are shown in Fig. 5. The values presented in Fig. 4 and Fig. 5 and were obtained for HCT, but the data obtained for RC were practically identical, so they have been omitted to avoid repetitive information. Fig. 6 presents the analytical and experimental values of the cooling temperature (T_r) versus the condensing pressure for both HCT and RC.

The comparison between analytical and experimental values of mass flow rates of the bleeding ($\dot{m}_{bd}$), cooling reflux ($\dot{m}_{cr}$), thermal power provided to the cycle ($\dot{Q}_{in}$), for both cycles and for the condensing and boiler pressures and steam mass flow rates indicated before are presented in Fig. 7 In the case of HCT, the mass flow rate of purges stream ($\dot{m}_p$) used for the different pressures of the boiler is presented in Fig. 7g.

The deviations between analytical and experimental values are all lower than 2.2%, being most of them lower than 1.2%. Therefore, analytical models provide values faithful to reality with a small margin of error. According to the results obtained in the plant, relative error in powers calculated were lower than 0.7%, also given a good accuracy for calculated results.

Fig. 8 presents the results of the mathematical model developed in this study and the data presented by the authors of [42] for the maximum flame temperature ($T_{fl,max}$) at different humidities and for the interval $1 \leq F_r \leq 1.2$. The discrepancies were lower than 1.7%. These results indicate that the model allows obtaining acceptable values for the influence of the air–fuel ratio in the boiler.

Table 1 shows the mass concentration of the different components of the purge stream. The total mass concentration of the hygroscopic compounds is 0.00215%.

With the values from Table 1 and according to Eq. (7) the specific chemical exergy of the purges stream (highest value of that magnitude in the cycle) was calculated for the base case. The value obtained was 0.00135 kJ/kg. It represents the 0.00035% of the total exergy of the purges (388.24 kJ/kg). Consequently, the chemical exergy of the working fluid is negligible in this study.

3.2. Comparison between HCT and RC (base case)

Fig. 9 and Fig. 10 show the T-s diagrams for the base case of HCT and regenerative RC respectively. Fig. 9 shows the different states of the working fluid for the HCT. Before the deaerator, point 8 reaches a temperature of 40 °C due to the heat recovery from the purges stream in the enthalpic recuperator. After that, the feedwater is preheated up to 103 °C in the deaerator. The Fig. 9 also includes a zoom of the zone of the condensate including the cooling reflux (points 13 and 14) to make it easier to distinguish the points as they are very close to each other on the initial scale. Fig. 10 represents the T-s diagram for the regenerative RC with deaerator. In that cycle, the temperature after the deaerator is 104 °C, but the mass flow rate extracted from the bleeding is greater than that of the HCT, consequently, the power produced by the turbine is greater for the HCT (Table 2 and Table 3) even with the extraction of mass flow rate due to the stream purges. Besides, the thermal power consumption in the boiler ($\dot{Q}_{in}$) of the HCT is lower than that of the regenerative RC (Table 4).

Table 2 and Table 3present the results of the exergy analysis for the base case. Exergy rates are shown in the form of Grassmann diagrams, presented in Fig. 11 and Fig. 12 for the RC and HCT respectively, including exergy destruction ratio (ϕ_i) of the equipment. Grassmann diagrams present the exergy percentage of the different streams with reference to the exergy rate of the fuel ($\dot{B}_{in}$) for each cycle. Note that necessary exergy rate of the fuel (Table 4) is lower for the HCT (37076 kW) than for the RC (37920 kW) to obtain the same useful exergy rate (10000 kW). From the results obtained, it can be concluded that the equipment with the highest exergy destruction (both absolute and
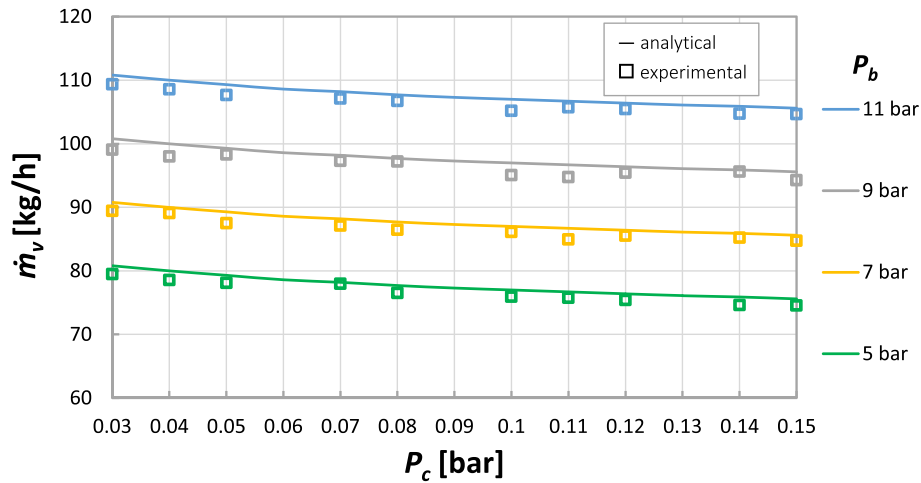
Fig. 4. Analytical and experimental values of the mass flow rate vs. the condensing pressure for different pressures in the boiler.
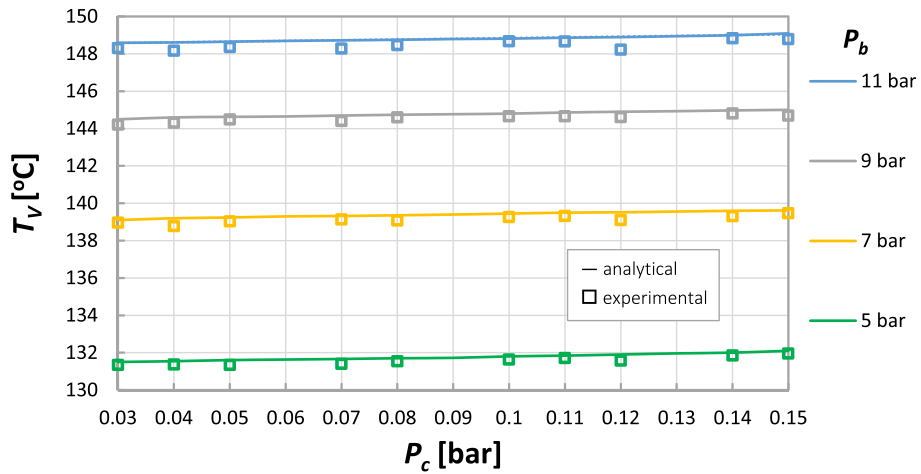

Fig. 5. Analytical and experimental values of the temperature of the vapor at the inlet of the condenser/absorber vs. the condensing pressure for different pressures in the boiler.
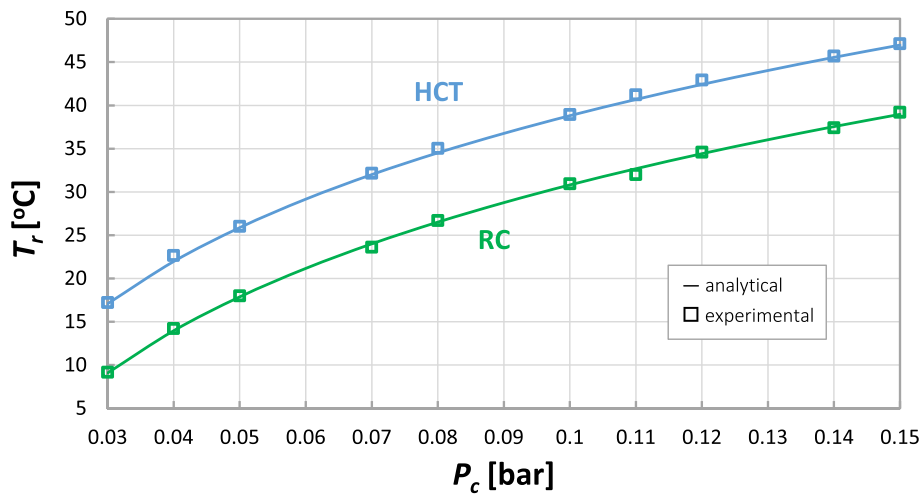

Fig. 6. Analytical and experimental values of the cooling temperature vs. the condensing pressure for HCT and RC.

relative) for the HCT is the boiler (63.0627%), the turbine (4.0526%), the dry coolers (2.0811%) and the absorber (1.0148%). In the case of the RC, the equipment with the highest irreversibilities is the boiler (62.9989%), the turbine (3.8718%), the dry coolers (2.1675%) and the condenser (2.0921%). Special emphasis should be placed on improving the design of equipment with higher irreversibilities. In the rest of the
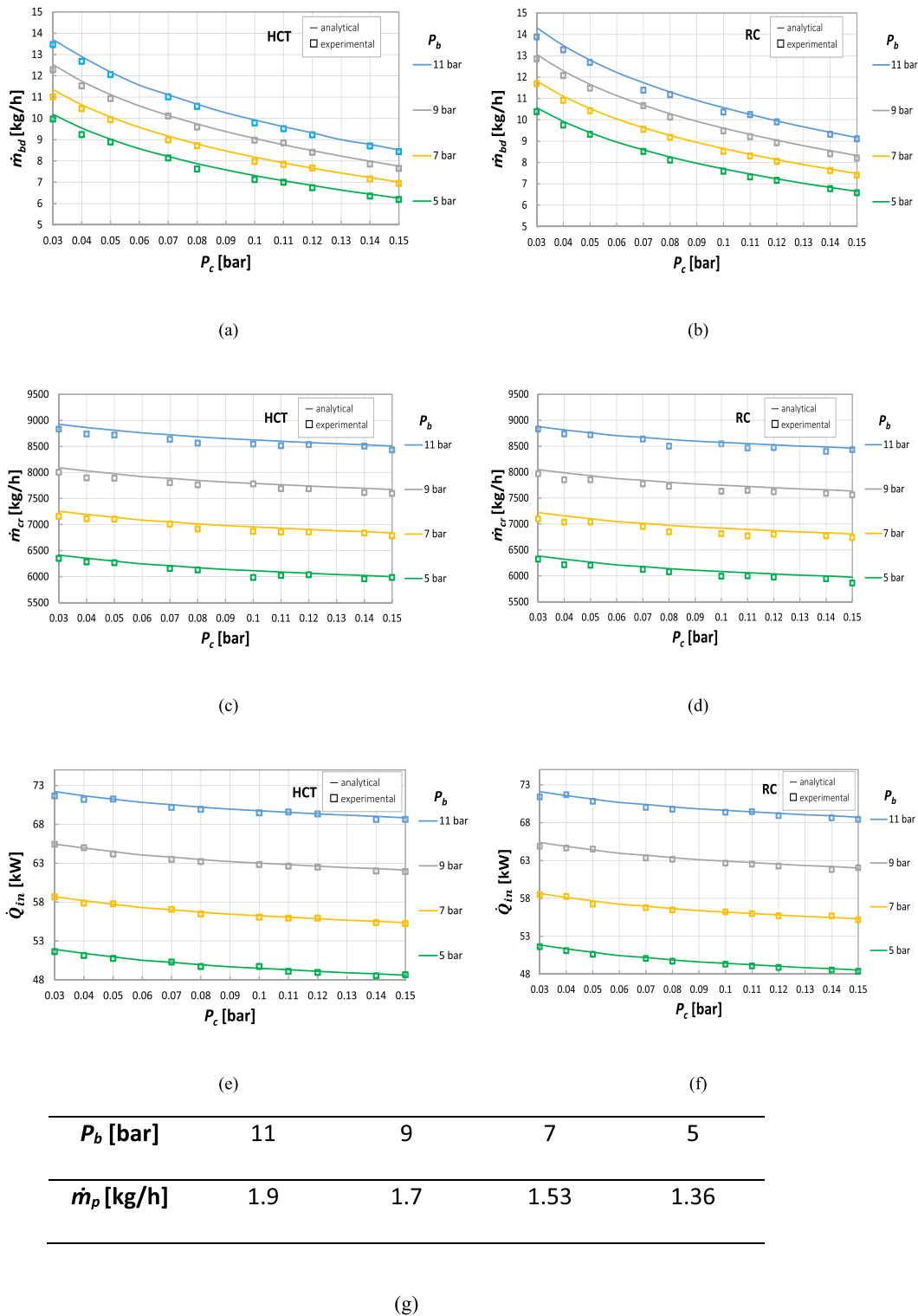
(a)

(b)

(c)

(d)

(e)

(f)

P_b [bar]	11	9	7	5
$\dot{m}_p$ [kg/h]	1.9	1.7	1.53	1.36

(g)

Fig. 7. Analytical and experimental values. (a) and (b): mass flow rate of the bleeding vs. condensing pressure for different pressures of the boiler (HCT and RC respectively); (c) and (d): mass flow rate of the cooling reflux vs. condensing pressure for different pressures of the boiler (HCT and RC respectively); (e) and (f): thermal power inlet vs. condensing pressure for different pressures of the boiler (HCT and RC respectively); (g) mass flow rate of purges stream for the different pressures of the boiler (HCT).

equipment the relative destruction of exergy is similar in both cycles and their percentages are quite small. As pointed out by [45] when the inlet and outlet temperatures of the fluid are similar in an equipment, the exergy destruction is reduced. That explains why the exergy destruction values are lower in those devices. It should be noted that in the HCT the enthalpic recuperator (a closed heat exchanger) is introduced, which is not included in the RC. Exergy inlet in the recuperator is the addition of the exergy of its 2 inlets and the percentage is relatively low (0.1798%), but half that exergy is destroyed in it (0.0917%). Consequently, the enthalpic recuperator is another element whose design should considered for improvement.

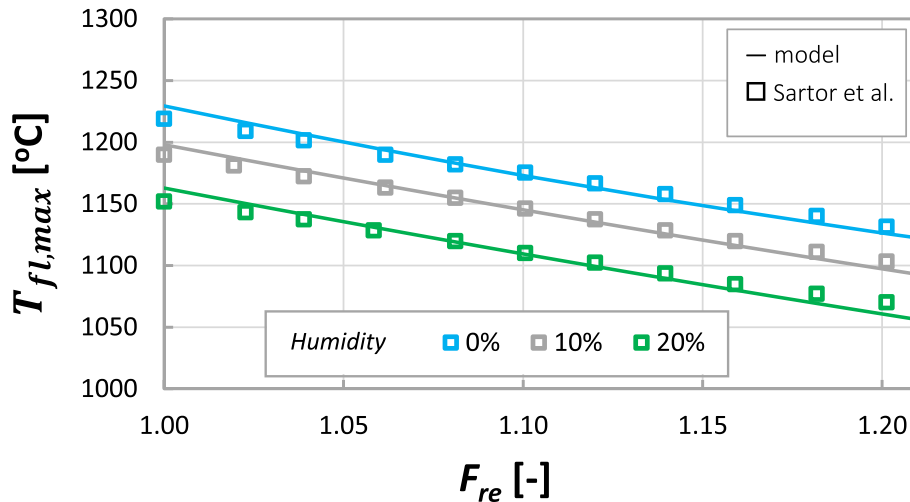The boiler is by far the equipment with the greatest irreversibilities.

Fig. 8. Comparison between the values obtained with the model of the boiler and the values obtained by [42] for the maximum flame temperature vs. relative air–fuel ratio with different humidity percentages of the biomass presented in [42].

Table 1
Mass concentration of the purge stream components.

Compound	Formula	Mass concentration (%)
Calcium carbonate	$CaCO_3$	0.001089
Nitrates	$[NO_3]^-$	0.00022
Nitrites	$[NO_2]^-$	0.0000055
Ammonium	$[NH_4]^+$	0.0000275
Chloride ions	$[Cl]^-$	0.000539
Fluoride ions	$[F]^-$	0.0000066
Sodium ions	$[Na]^+$	0.000264
Water	H_2O	99.99785

Those irreversibilities represent a percentage of 63.06% and 63.00% for the HCT and RC respectively (with reference to their corresponding exergy rate of the fuel). Most of the exergy destruction occurs in combustion since chemical reactions produce high irreversibilities [45]. According to Grassmann diagrams, the exergy balance in the deaerator of both cycles is almost identical with an exergy destruction ratio of about 0.40%.

As mentioned above, the absorber presents a relatively elevated rate of irreversibilities. The greatest entropy generation in the absorber is due to the mixing of two different fluids [46], in this case, the pure steam stream and a mixture of water and hygroscopic compounds. However, the exergy destruction rate in the RC condenser, working at the same cooling temperature as in the HCT, is about twice as much as in the absorber.

The turbines of both cycles have a noticeable exergy destruction, compared to other equipment. In high-pressure steam expansion, almost twice as much power is produced as in low-pressure expansion for both HCT and RC (Table 2 and Table 3). Irreversibilities of the turbines are also higher at high-pressure stage. Dry coolers work properly when the cooling temperature is at least 6 °C higher than the ambient temperature. In this extreme case, which is the one being studied, the entire the whole set of fans of the dry coolers is in operation, being their consumption maximum and dry coolers of both cycles behave similarly. According to Grassmann diagrams the percentages of exergy rate are similar in the dry coolers of HCT and RC, but exergy destruction and exergy consumption rate of the fans is lower in the HCT than in RC. In the case of the pumps, the self-consumption rate is higher in the HCT than in the RC. The condensate pump of the HCT has a notable consumption since it works with a much higher cooling flow rate than the condensate pump of the RC. For the base case, exergy destruction percentage of the condensate pump is 0.0837% for the HCT, and 0.0019% for the RC. According to Table 2 and Table 3, the power consumption is respectively 31.04 kW and 0.728 kW. All that is due to the different mass flow rate of the condensate as a consequence of the different layout of the cycles. In the case of the HCT the condensate mass flow rate is very high (1.35 t/h), because it includes the cooling reflux (1.31 t/h), while for the RC, the mass flow rate of the condensate is much lower (0.033 t/h), and the cooling mass flow rate (1.37 t/h) belongs to a different loop. According to Plojak et al. [47], when increasing the mass flow rate of the pump, the exergy losses are also increased. Note that despite that fact, the exergy efficiency of the HCT is higher than the one of the RC.

In the HCT the cooling reflux is used for refrigeration instead of cooling water and cooling pump is not needed. Furthermore, the exergy losses associated with other elements are higher in the HCT, since it
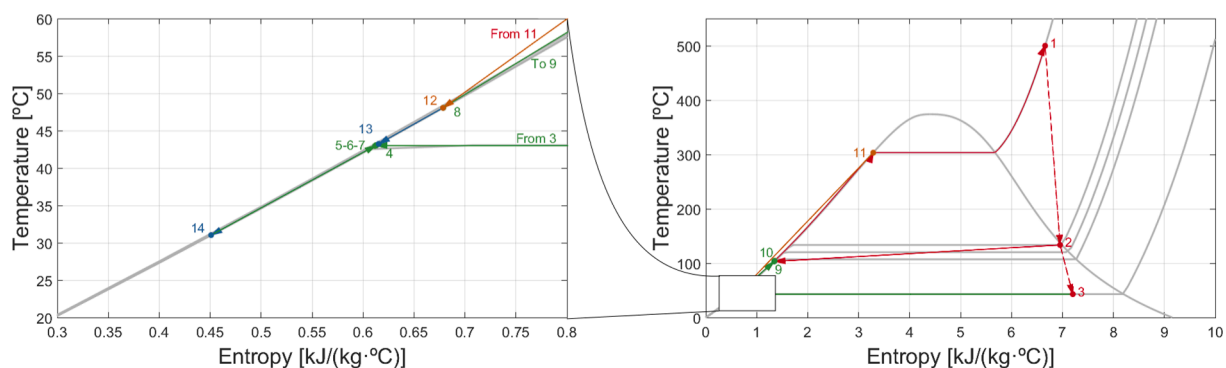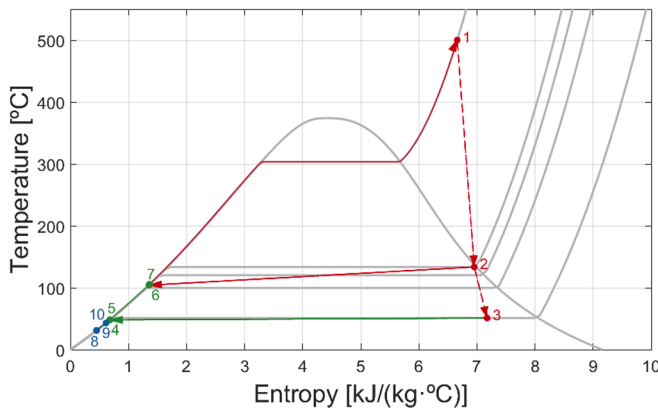

Fig. 9. T-s diagram of HCT.

Fig. 10. T-s diagram of RC.

Table 2
Exergy analysis of the HCT.

Element	$\Delta\dot{B}$(kW)	$\dot{B}_{\dot{Q}}$(kW)	$\dot{B}_{\dot{W}}$(kW)	$\dot{B}_d$(kW)
Absorber	376.26	0.00	0.00	376.26
Condensate pump	−112.10	0.00	−143.14	31.04
Recuperator	33.998	0.00	0.00	33.998
Deaerator	150.09	0.00	0.00	150.09
Feed water pump	−102.50	0.00	−125.30	22.80
Boiler	23381.11	0.00	0.00	23381.11
High-pressure turbine	7427.00	0.00	6577.00	850.00
Low-pressure turbine	4573.10	0.00	3920.54	652.56
Dry coolers	750.24	−207.74	−229.10	771.60
Valves, nodes, pressure loss	161.558	0.00	0.00	161.558
Total	36638.756	−207.74	10000.00	26431.016

Table 3
Exergy analysis of the RC.

Element	$\Delta\dot{B}$(kW)	$\dot{B}_{\dot{Q}}$(kW)	$\dot{B}_{\dot{W}}$(kW)	$\dot{B}_d$(kW)
Condenser	793.36	0.00	0.00	793.36
Condensate pump	−2.684	0.00	−3.412	0.728
Deaerator	151.98	0.00	0.00	151.98
Feed water pump	−103.90	0.00	−127.02	23.12
Boiler	23889.20	0.00	0.00	23889.20
High pressure turbine	7646.10	0.00	6770.00	876.10
Low pressure Turbine	4241.00	0.00	3648.93	592.07
Dry coolers	775.78	−192.80	−238.898	821.878
Cooling pump	−38.38	0.00	−49.60	11.22
Valves, pressure loss	110.55	0.00	0.00	110.55
Total	37463.006	−192.80	10000.00	27270.206

Table 4
Thermal and exergy efficiencies, input thermal power, useful exergy rate and exergy rate of the fuel for HCT and RC (base case).

Cycle	η_t(%)	η_{ex}(%)	$\dot{Q}_{in}$(kW)	$\dot{B}_u$(kW)	$\dot{B}_{in}$(kW)
HCT	34.84	26.97	28,700	10,000	37,076
RC	34.07	26.37	29,354	10,000	37,920

works with three more valves and there are two nodes that are not present in the RC. Despite all this, thermal and exergy efficiency are greater in the case of HCT. Table 4 shows the thermal and exergy efficiencies of the HCT and the RC for the base case. According to those results, HCT has a thermal efficiency that is 2.26% greater than that of the RC. The exergy efficiency of the HCT is 2.28% greater than that of the RC. This improvement in performance is mostly due to the fact that the HCT operates at lower condensing pressures than the RC for the same cooling temperature and, consequently, since the net power

produced is the same, the power consumed in the boiler of the HCT is lowered. It should be considered that for an ambient temperature of 25 °C the RC is still comparable with the HCT, since for this case the cooling can be done by dry process in the RC. The HCT ensures dry cooling of the exhaust steam with a low consumption of energy at the dry coolers while for the RC, water cooling systems such as cooling towers are needed for high ambient temperatures. In addition, the HCT presents fewer total irreversibilities, which translates into better utilization of input exergy and, therefore, a higher net exergy efficiency. The increase in exergy efficiency in the HCT is favored, partly, by the utilization of the energy from the boiler blowdowns stream to preheat the feedwater. The improvement in both thermal and exergy efficiency of HCT is achieved without the need for water consumption for refrigerating the cycle, so that water cooling systems, including cooling towers, can be eliminated.

3.3. Analysis of the boilers for the base case

Once the general analysis for both cycles is done, a specific analysis of the boilers is presented. Common data for the base case of the adiabatic stoichiometric combustion is presented in Table 5.

Particular data for combustion in the cycles are compared in Table 6.

The thermal efficiency of the boiler is slightly greater in the HCT than in the RC. The HCT boiler needs to consume less thermal energy than the RC boiler for the same net power output in the plant. That translates into lower fuel consumption and, consequently, economic savings. Exergy destruction ratio is slightly greater in the HCT boiler than in RC boiler and consequently, the exergy efficiency is slightly lower in the HCT (note that part of the exergy is extracted by the purges stream).

Table 7 shows the temperatures of the flue gases and the working fluid in the boilers of both cycles, according to Fig. 3. T_1 to T_3 are the temperatures of the flue gas and T_a to T_d are the temperatures of the working fluid in the boilers. According to Table 7, the working fluid has practically the same temperature distribution in both boilers, while the temperatures of the flue gas are greater in the boiler of the HCT than the RC. Fig. 13 and Fig. 14 show the Grassmann diagrams of the two boilers in more detail, considering both the combustion process and the heat transfer exchange separately. In the combustion process most of the boiler exergy destruction occurs, both for HCT and RC, being no difference in the destruction ratio between both cycles. The heat exchange of the flue gas with the working fluid is another source of irreversibilities (external irreversibilities) because of the difference between flue gas and feedwater temperature. Exergy destruction rate during the heat exchange is greater in the HCT than in the RC, mainly due to the greater difference of temperature between the flue gases and the working fluid (Table 7). Finally, there are some losses associated with the fumes (same exergy rate percentage for both cycles). That exergy could be potentially recovered to preheat the boiler feed air, which would lead to an increase in exergy efficiency since the air would require less energy to be heated to the combustion temperature.

3.4. Sensitivity analysis

In the sensitivity analysis, HCT and RC are compared maintaining the same cooling temperature in both cycles as in the base case. The variables considered for the analysis are the condensing pressure, cooling temperature, ambient temperature, temperature difference of the working fluid in the dry coolers, bleeding pressure, temperature and pressure at the outlet of the boiler, and relative air–fuel ratio. Each of these variables is varied one by one (keeping the rest of the values of the other variables constant as in the base case) in order to obtain the relationships among them and their influence on the thermal power demand, thermal and exergy efficiencies, and exergy destruction ratio in the boiler.

In this study the values of condensing pressure tolerable by the turbine range from 0.05 to 0.24 bar [24,48]. Fig. 15 shows how the
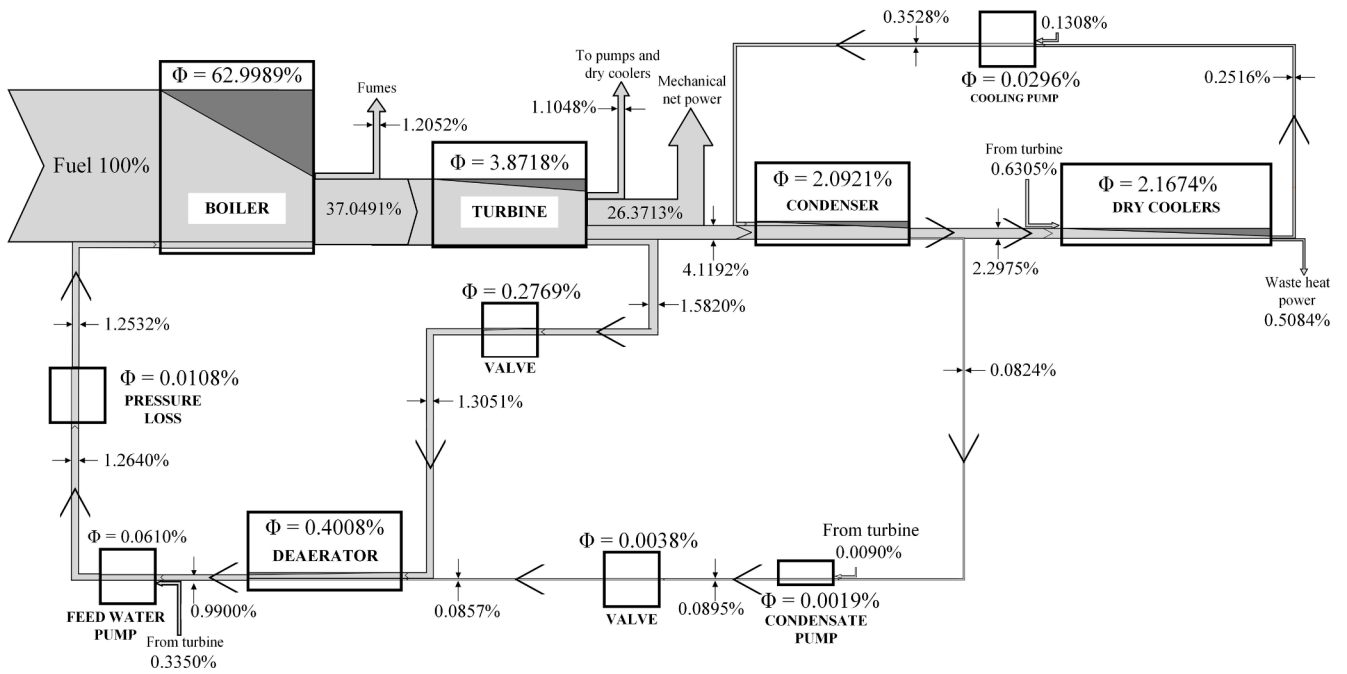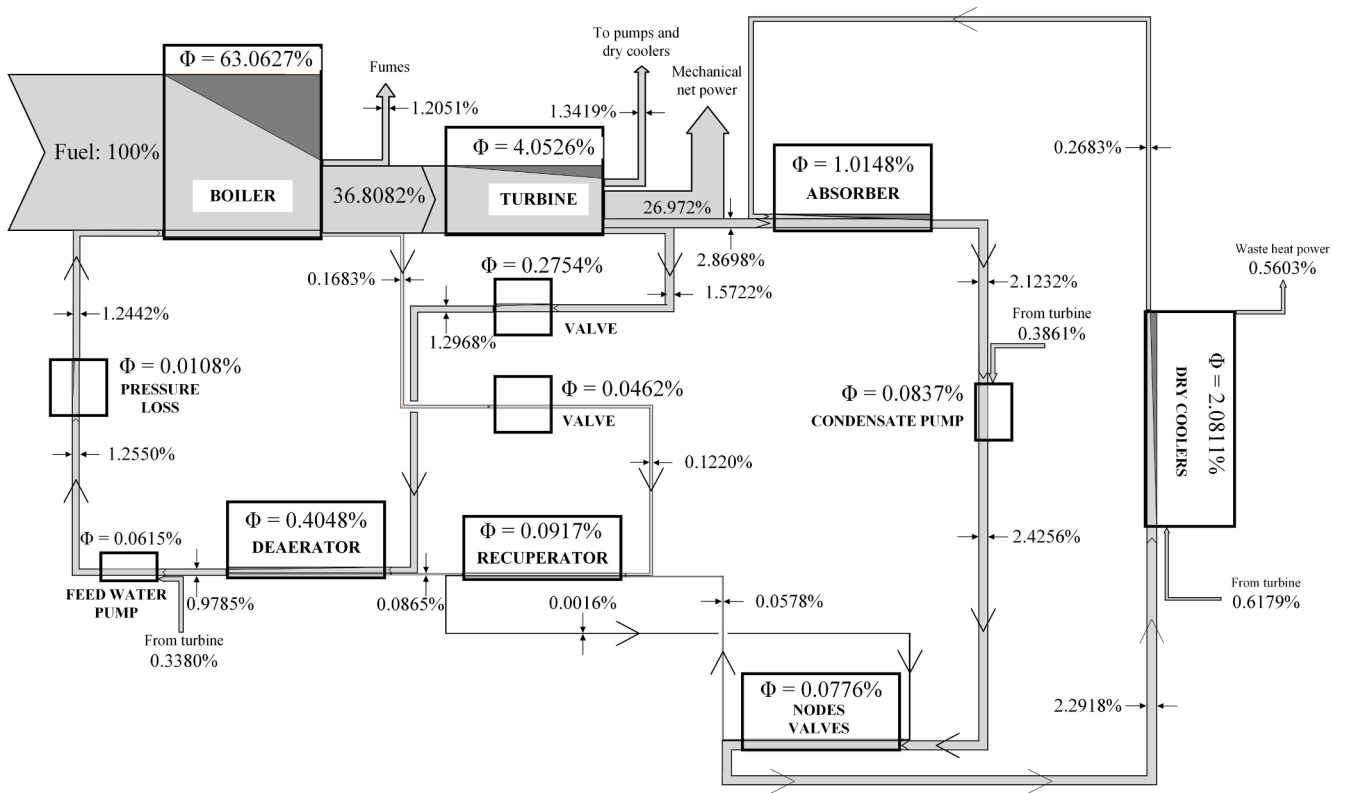
Fig. 11. Grassmann diagram of the RC.

Fig. 12. Grassmann diagram of the HCT.

Table 5
Common combustion date for the HCT and RC.

Molecular mass of alperujo (kg/kmol)	22.85
Molecular mass of combustion gases (kg/kmol)	29.17
β (dimensionless)	1.121
Adiabatic flame temperature (°C)	1654

Table 6
Particular data of combustion for the HCT and RC.

Cycle	$\dot{m}_f$(kg/s)	$\dot{m}_{air}$(kg/s)	$\dot{m}_{fumes}$(kg/s)	$\eta_{t,b}$(%)	$\eta_{ex,b}$(%)	Φ_b(%)
HCT	2.14	11.60	13.74	73.50	35.74	63.05
RC	2.19	11.86	14.05	73.46	35.79	63.00

Table 7

Temperatures of gases and working fluid in the boilers of HCT and RC.

Cycle	T_1(°C)	T_2(°C)	T_3(°C)	T_a(°C)	T_b(°C)	T_c(°C)	T_d(°C)
HCT	950.0	646.8	160.0	104.0	298.3	303.3	500.0
RC	946.1	640.5	160.0	105.0	298.3	303.3	500.0

condensing pressure of HCT and RC varies when cooling temperature ranges from 20 to 52 °C. According to those results, condensing pressure is greater for the RC than HCT for maintaining the same cooling temperature, and the difference between the condensing pressures increases as the cooling temperature increases. Consequently, the power produced in the turbine is greater for HCT than RC as cooling temperature is increased. Notice that the minimum difference between condensing temperature and ambient temperature is 6 °C to ensure a correct functioning of the dry coolers. According to Fig. 15, at the maximum condensing pressure (0.24 bar) the cooling temperature is 44 °C for the RC, therefore, the maximum ambient temperature at which dry coolers can be used for cooling in the RC is 38 °C, while for HCT, dry coolers can be used up to ambient temperatures of 46 °C (cooling temperature of 52 °C).

Fig. 16 and Fig. 17 present the thermal and exergy efficiencies of both HCT and RC with dry coolers at different cooling temperatures. Both efficiencies decrease in both cycles as cooling temperature rises. In the case of RC, when ambient temperature reaches temperatures over 38 °C (cooling temperature of 44 °C) dry coolers are not capable of refrigerate and it is necessary to use cooling towers [24]. Therefore, under those conditions the layout of the RC changes, the consumption of the refrigeration system is greater than that of the dry coolers and the cycles are not comparable, being HCT far superior, and RC efficiencies are much lower than for the HCT. According to those results, exergy efficiency of the HCT is 2.21% greater than that of the RC, increasing that improvement when cooling temperature is increased, and reaching values greater than 2.52%.

Fig. 18 shows the variation of thermal and exergy efficiencies for HCT and RC for temperature differences between inlet and outlet of the dry cooler (ΔT_{dc}) ranging from 5 °C to 14 °C. Also, the cooling
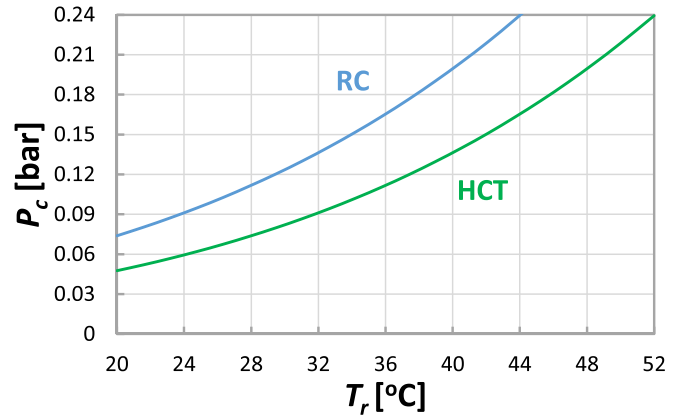

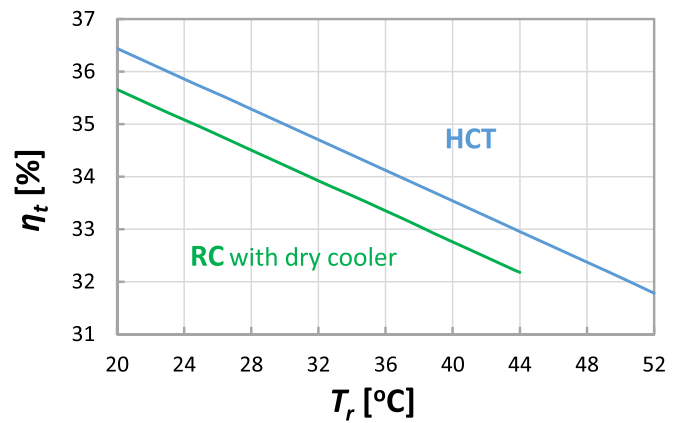**Fig. 15.** Condensing pressure vs. cooling temperature for HCT and RC.

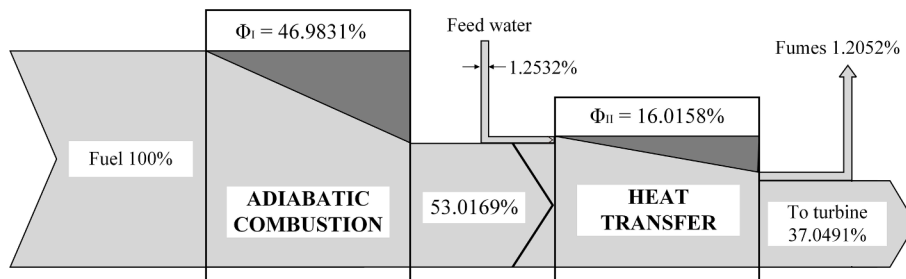**Fig. 16.** Thermal efficiency vs. condensing temperature for HCT and RC with dry cooler.

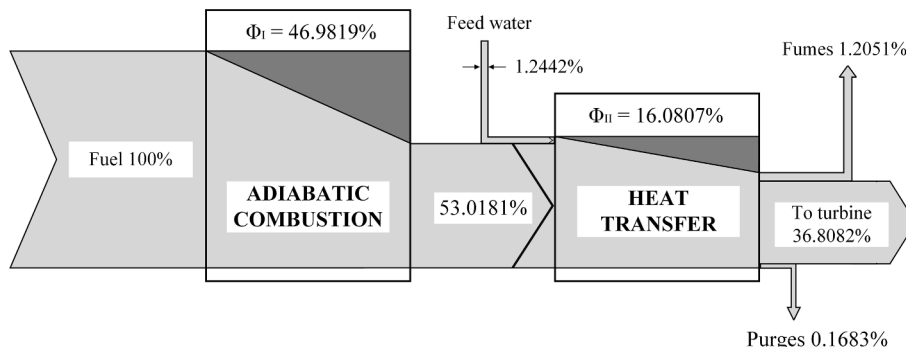**Fig. 13.** Grassmann diagram of the RC boiler.

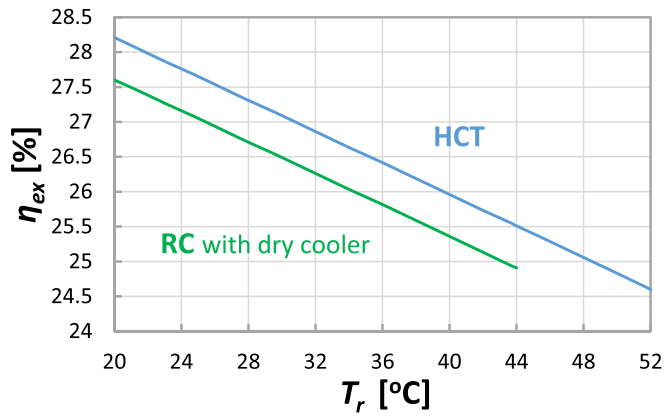**Fig. 14.** Grassmann diagram of the HCT boiler.

Fig. 17. Exergy efficiency vs. cooling temperature for HCT and RC.

Fig. 19. Thermal and exergy efficiencies and thermal power input vs condensing pressure.

temperature for each case is plotted in the figure. The total increments in the interval studied are of 0.77% and 0.76% in thermal and exergy efficiency respectively for the RC. However, the effect is much more significant in the HCT because the increments are of 2.20% and 2.23% in thermal and exergy efficiency respectively.

3.4.1. Sensitivity analysis of the HCT

After comparing the two cycles, a more detailed sensitivity analysis of the HCT is presented. Fig. 19 displays the decrease in both thermal and exergy efficiencies of the HCT when increasing condensing pressure (P_c). When condensing pressure is raised the pressures at the inlet and outlet of the turbine become closer. In order to maintain the net power produced, mass flow rate and thermal power supplied to the cycle in the boiler has to be increased (Fig. 20). Therefore, thermal efficiency decreases. For the exergy efficiency the trend is the same as for thermal efficiency, as the condensing pressure increases the exergy efficiency decreases. The decrease in efficiencies is very significant when condensing pressure is raised (efficiencies are 12.6% lower and thermal demand is 15.4% higher for 0.24 bar than for 0.05 bar). Therefore, it is more beneficial to set condensing pressure as low as possible, since this leads to a better use of the energy and exergy input to the cycle.

The results show that when the bleeding pressure is increased from 2 bar to 20 bar, both thermal and exergy efficiencies of the HCT decrease by 2.4% and the inlet thermal power decreases by 2.5% (Fig. 20). Consequently, an adequate value of the bleeding pressure is between 2 bar and 4 bar to assume the variations due to different operating conditions. Fig. 20 also shows how thermal power required by the cycle is increased when bleeding pressure is raised. The increase in thermal power demanded is more pronounced for the lower values of the studied
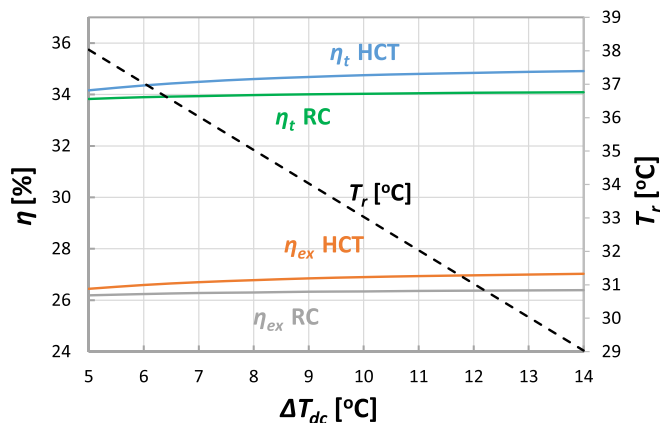
range. Since the net power in fixed the decrease of the efficiencies is also more pronounced in that range. Considering a nominal value of 3 bar for the bleeding pressure, variations in the interval from 2 bar to 4 bar yield to variations of 0.1% in the efficiencies.

Figs. 21 and 22 show the variation of thermal and exergy efficiencies and thermal power demanded when pressure (P_b) and temperature (T_{max}) at the outlet of the boiler are increased respectively. The effect of both variables is similar and represents a maximum decrease of 7.4% in thermal power input and a maximum increase of the efficiencies of 7.7% in the wide range studied. Consequently, the more significant effect in the efficiencies is due to the condensing pressure.

Fig. 20. Thermal and exergy efficiencies and thermal power input vs bleeding pressure.

Fig. 18. Thermal and exergy efficiency vs. temperature difference of the working fluid in the dry coolers for HCT and RC.
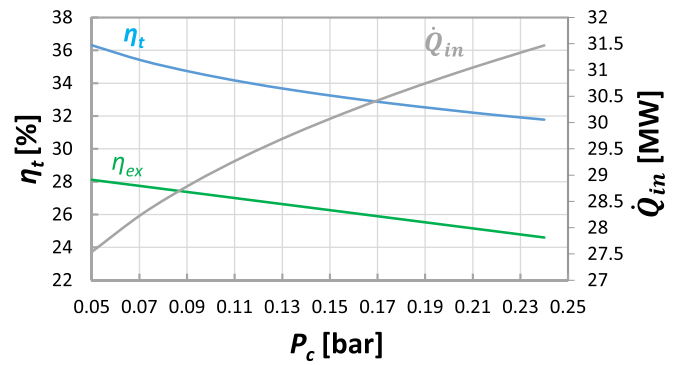

Fig. 21. Thermal and exergy efficiencies and thermal power input vs boiler pressure.
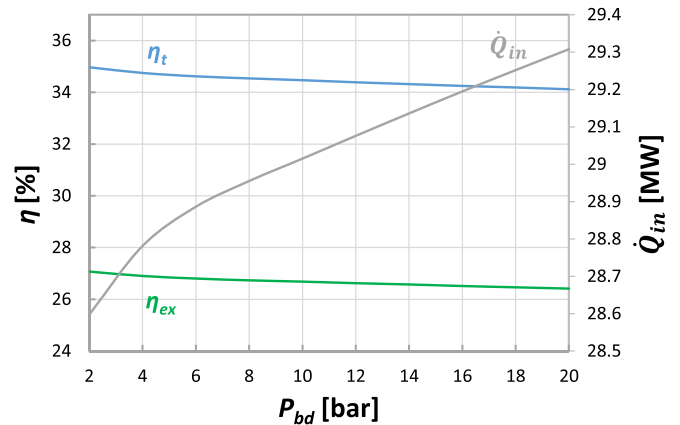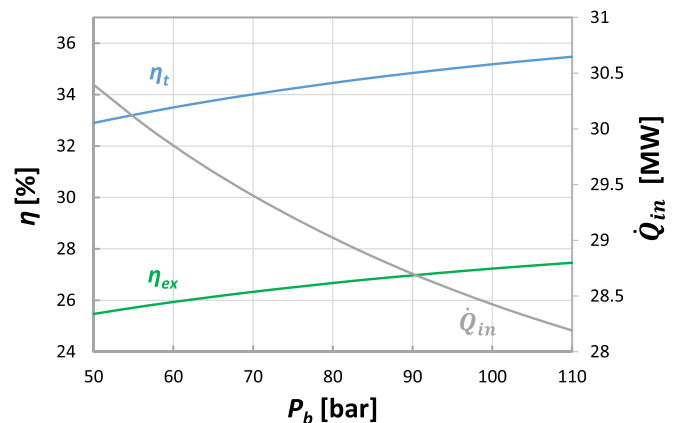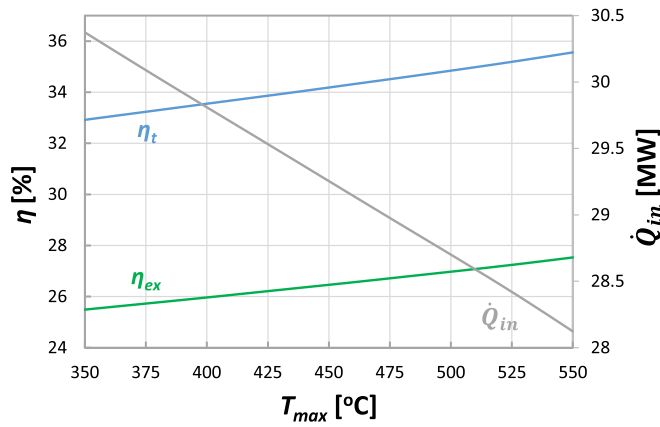
Fig. 22. Thermal and exergy efficiencies and thermal power input vs maximun temperature of the working fluid.

The boiler presents the largest exergy losses of the cycle. The effect of excess of air in the exergy destruction ratio of the boiler is presented in Fig. 23 for a cooling pressure of 0.0865 bar (25 °C ambient temperature). At a relative air–fuel ratio of 1.2, the exergy destruction can reach a value of 63.7%, an increase of 1% with reference to the stoichiometric air–fuel ratio. This is due to the fact that the air consumes part of the energy given off in combustion, so more energy is needed. The relationship between exergy destruction and air–fuel ratio is practically linear.

As the air–fuel ratio increases, the exergy destruction in the boiler increases and also the exergy efficiency of the HCT decreases. Fig. 23 shows the influence of the boiler on the operation of the cycle and highlights the need to optimize its operating conditions. As the exergy destruction in the boiler is increased by operating at higher air–fuel ratios, the exergy efficiency of the HCT decreases from 26.97% (stoichiometric) to values slightly above 26.6% (1.3% lower) over the interval studied.

4. Conclusions

An analytical model of the proprietary cycle called Hygroscopic cycle (HCT) has been developed and validated with experimental data provided in a pilot power plant. Also, an analytical model of the regenerative Rankine cycle has been developed in order to compare both cycles under different working conditions at industrial scale. The article aims to analytically study and compare their performance based on energy and exergy analysis including both chemical and physical exergy of the cycles.

A base case of each cycle is defined and compared, and a sensitivity analysis of the main variables and parameters involved in the cycles has been done. Also, Grassman diagrams of both cycles for the base cases
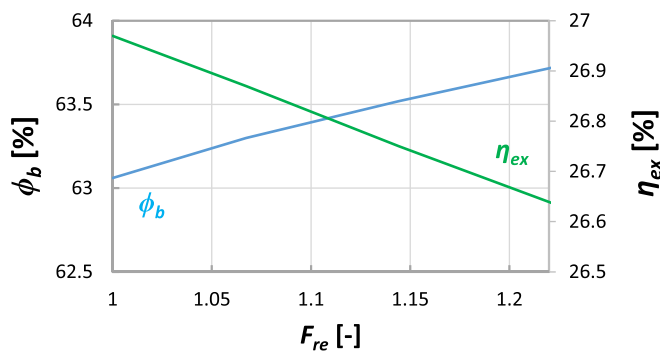

Fig. 23. Exergy destruction ratio in the boiler and exergy efficiency of the HCT vs relative air–fuel ratio.

have been presented and analyzed in order to quantify the exergy distribution and the exergy destruction.

The HCT has been compared with the analytical model of the regenerative RC keeping constant the cooling temperature at 31 °C and other operating parameters (net power, boiler pressure, maximum temperature of the boiler, etc.) for the base case.

The results show that the exergy efficiency of the HCT is, in relative terms, 2.2% higher than that of the regenerative RC and the thermal efficiency is 2.26% higher for the base case. In other words, the HCT makes better use of the input exergy. In addition, fuel consumption is reduced, since the thermal power needed the boiler is reduced. Lower fuel consumption means lower emissions of polluting gases. That, together with the savings in cooling water make the HCT an environmentally friendly technology necessary for the energy transition.

Regarding the destruction of exergy in each device in the HCT for the base case, the equipment with the greatest irreversibilities is the boiler, the turbine, the absorber and dry coolers. In these four units, almost 70% of the exergy is destroyed. For the RC base case, the most inefficient ones are the boiler, the turbine, the condenser and the dry coolers, devices in which over 70% of the input exergy is destroyed. Of the abovementioned equipment, the most inefficient one is the boiler.

A detailed energy and exergy study of the base case boilers that use alperujo as fuel, biomass widely used in existing HCT power plants at industrial scale, is presented. Exergy destruction ratio is slightly greater in the HCT boiler (63.06%) than in RC boiler (63.00%) and consequently, the exergy efficiency of the boiler is slightly lower in the HCT (35.74%) than RC (35.79%). The difference is mainly due to external irreversibilities in the heat exchange between the flue gas and the working fluid in the boiler.

The analysis was performed for a 10 MW power plant in all cases and the exergy of the fuel in absolute terms was lower for the HCT (37.08 MW) than for the RC (37.92 MW). The absorber turns out to be a more efficient equipment, in terms of exergy, than the condenser, since approximately exergy destruction in the absorber is half than in the condenser.

From the sensitivity analyses carried out, it can be concluded that the variables that have the greatest influence on the exergy efficiency are the condensing pressure and the boiler air–fuel ratio. The results indicate that for variations of the bleeding pressure due to different operating conditions give rise to variations up to 0.1% in the efficiencies.

For the range of condensing pressures studied (0.5 bar to 0.24 bar) the maximum ambient temperature at which dry coolers can be used for cooling in the RC is 38 °C, while for HCT, dry coolers can be used up to ambient temperatures of 46 °C and exergy efficiency of the HCT reaches values over 2.52% greater than RC. For ambient temperatures higher than 38 °C the RC is to be refrigerated with cooling towers and, consequently, with water consumption.

The lower the condensing pressure, the higher the exergy efficiency (even up to 26% for the HCT), because if the net power is kept constant, the exergy to be delivered is minimized as well as the heat to be evacuated in the dry coolers. However, if it is necessary to work at high ambient temperatures, the condensing pressure must be increased.

The condensing pressure of the RC is greater than that of the HCT for the same cooling temperature. Considering the same cooling temperature and the same turbine inlet conditions in both cycles, the specific work of the turbine will be lower in the case of RC. This effect also contributes to the fact that the HCT has a higher efficiency than the RC.

HCT operates up to cooling temperatures of 52 °C (maximum ambient temperature of 46 °C). This value is achieved for the maximum tolerable pressure in the turbine. Consequently, the HCT is able of working at high ambient temperatures without the need to consume cooling water. However, increasing the cooling temperature (or the condensing pressure) leads to an increase in the thermal power that must be dissipated in the dry coolers, which implies higher power consumption and a reduction in thermal and exergy efficiencies.

The maximum ambient temperature for the dry coolers to operate

properly is more limited in the RC. This is one of the great advantages of the HCT, since it allows to increase the operating hours of the plant in regions where the ambient temperature is very high. The HCT can be designed to operate at the maximum ambient temperature of the region where the plant is to be installed. It is also possible to modify Rankine cycle plants by incorporating the HCT cycle to increase the availability factor of the plant.

Excess air in the boiler has a negative influence on the exergy destruction of the boiler. For the HCT with a relative air–fuel ratio of 1.2, the exergy destruction rate in the boiler increases up to 63.7%, an increase of 1% with respect to the stoichiometric air–fuel ratio. Also, the exergy efficiency of the HCT decreases to about 26.6%, which is 1.3% lower than the value for the stoichiometric ratio. That effect could be alleviated by using the heat from the boiler exhaust fumes to preheat the feed air.

CRediT authorship contribution statement

Malena Potesta González: Conceptualization, Software, Writing – original draft. **Roberto Martínez-Pérez:** Methodology, Data curation. **Andrés Meana-Fernández:** Writing – review & editing, Validation. **Francisco J. Rubio-Serrano:** Resources, Validation. **Antonio J. Gutiérrez-Trashorras:** Supervision, Project administration.

Declaration of Competing Interest

The authors declare that they have no known competing financial interests or personal relationships that could have appeared to influence the work reported in this paper.

Data availability

Only the data presented in the article will be available

Acknowledgments

References

[1] Zakeri B, Paulavets K, Barreto-Gomez L, Echeverri LG, Pachauri S, Boza-Kiss B, et al. Pandemic, War, and Global Energy Transitions. Energies 2022;15(17):6114.

[2] International Energy Agency. Word Energy Outlook 2022. Accessed June 2023, https://iea.blob.core.windows.net/assets/c282400e-00b0-4edf-9a8e-6f2ca6536ec8/WorldEnergyOutlook2022.pdf; October 2022.

[3] Dincer I, editor. Comprehensive energy systems. Elsevier; 2018.

[4] Sarr JAR, Mathieu-Potvin F. Increasing thermal efficiency of Rankine cycles by using refrigeration cycles: a theoretical analysis. Energ Conver Manage 2016;121:358–79.

[5] Çengel YA, Boles MA. Termodinámica. México: McGraw Hill; 2014.

[6] Loni R, Najafi G, Bellos E, Rajaee F, Said Z, Mazlan M. A review of industrial waste heat recovery system for power generation with Organic Rankine Cycle: Recent challenges and future outlook. J Clean Prod 2021;287:125070.

[7] Kang SH. Design and experimental study of ORC (organic Rankine cycle) and radial turbine using R245fa working fluid. Energy 2012;41(1):514–24.

[8] Li X, Xu B, Tian H, Shu G. Towards a novel holistic design of organic Rankine cycle (ORC) systems operating under heat source fluctuations and intermittency. Renew Sustain Energy Rev 2021;147:111207.

[9] Thurairaja K, Wijewardane A, Jayasekara S, Ranasinghe C. Working fluid selection and performance evaluation of ORC. Energy Procedia 2019;156:244–8.

[10] Xu W, Zhao R, Deng S, Zhao L, Mao SS. Is zeotropic working fluid a promising option for organic Rankine cycle: A quantitative evaluation based on literature data. Renew Sustain Energy Rev 2021;148:111267.

[11] Tian Z, Zeng W, Gu B, Zhang Y, Yuan X. Energy, exergy, and economic (3E) analysis of an organic Rankine cycle using zeotropic mixtures based on marine engine waste heat and LNG cold energy. Energ Conver Manage 2021;228:113657.

[12] Júnior EPB, Arrieta MDP, Arrieta FRP, Silva CHF. Assessment of a Kalina cycle for waste heat recovery in the cement industry. Appl Therm Eng 2019;147:421–37.

[13] Mergner H, Weimer T. Performance of ammonia–water based cycles for power generation from low enthalpy heat sources. Energy 2015;88:93–100.

[14] Köse Ö, Koç Y, Yağlı H. Is Kalina cycle or organic Rankine cycle for industrial waste heat recovery applications? A detailed performance, economic and environment based comprehensive analysis. Process Saf Environ Prot 2022;163:421–37.

[15] Demirkaya G, Vasquez Padilla R, Fontalvo A, Lake M, Lim YY. Thermal and exergetic analysis of the Goswami cycle integrated with mid-grade heat sources. Entropy 2017;19(8):416.

[16] Demirkaya G, Padilla RV, Fontalvo A, Bula A, Goswami DY. Experimental and theoretical analysis of the Goswami cycle operating at low temperature heat sources. J Energy Res Technol 2018;140(7).

[17] Fontalvo A, Pinzon H, Duarte J, Bula A, Quiroga AG, Padilla RV. Exergy analysis of a combined power and cooling cycle. Appl Therm Eng 2013;60(1–2):164–71.

[18] Singh A, Das R. A novel combined power and cooling cycle design and a modified conditional exergy destruction approach. Energ Conver Manage 2021;233:113943.

[19] Hu S, Li J, Yang F, Yang Z, Duan Y. How to design organic Rankine cycle system under fluctuating ambient temperature: A multi-objective approach. Energ Conver Manage 2020;224:113331.

[20] Fernandez DAP, Foliaco B, Padilla RV, Bula A, Gonzalez-Quiroga A. High ambient temperature effects on the performance of a gas turbine-based cogeneration system with supplementary fire in a tropical climate. Case Stud Therm Eng 2021;26:101206.

[21] Sun Z, Liu C, Xu X, Li Q, Wang X, Wang S, et al. Comparative carbon and water footprint analysis and optimization of Organic Rankine Cycle. Appl Therm Eng 2019;158:113769.

[22] Macknick J, Newmark R, Heath G, Hallett KC. Operational water consumption and withdrawal factors for electricity generating technologies: a review of existing literature. Environ Res Lett 2012;7(4):045802.

[23] Rubio-Serrano, F.J. Ciclo Higroscópico. https://www.ciclohigroscopico.com/. (Accessed June 2023).

[24] Rubio-Serrano FJ, Gutiérrez-Trashorras AJ, Soto-Pérez F, Álvarez-Álvarez E, Blanco-Marigorta E. Advantages of incorporating Hygroscopic Cycle Technology to a 12.5-MW biomass power plant. Appl Therm Eng 2018;131:320–7.

[25] Martínez-Pérez R, Rubio-Serrano FJ, Meana-Fernández A, Gutiérrez-Trashorras AJ. Influence of LiBr concentration in the generation of superheated vapor for a Hygroscopic Cycle. Renew Energy Power Quality J 2022.

[26] Martínez-Pérez R, Peris-Pérez B, Ríos-Fernández JC, González-Caballín JM, Rubio-Serrano F, Trashorras AJG. Analytical Model of the Refrigeration System for Cooling in a Hygroscopic Cycle Power Plant. 21th International Conference on Renewable Energies and Power Quality (ICREPQ'23). Madrid (Spain), 24th to 26th May 2023.

[27] Rubio-Serrano FJ, Soto-Pérez F, Gutiérrez-Trashorras AJ. Influence of cooling temperature increase in a hygroscopic cycle on the performance of the cooling equipment. Energ Conver Manage 2019;200:112080.

[28] Serrano FJR, Pérez FS, Trashorras AJG, Abad GA. Comparison between existing Rankine Cycle refrigeration systems and Hygroscopic Cycle Technology (HCT); 2018.

[29] Rubio-Serrano FJ, Soto-Perez F, Gutierrez-Trashorras AJ. Experimental study on the influence of the saline concentration in the electrical performance of a Hygroscopic cycle. Appl Therm Eng 2020;165:114588.

[30] Larsen MAD, Drews M. Water use in electricity generation for water-energy nexus analyses: The European case. Sci Total Environ 2019;651:2044–58.

[31] IMATECH, *IMASA Technologies.* https://imasatechnologies.com/. (Accessed June 2023).

[32] Oleícola el Tejar, *Oleícola el Tejar.* https://eltejar.sbsoftware.es/. (Accessed June 2023).

[33] Moran MJ, Sciubba E. Exergy analysis: principles and practice. J Eng Gas Turbines Power 1994;1(2):285–90.

[34] Fitouri H, Jeday M-R, Hajjaji N. A comprehensive exergy analysis of a propylene refrigeration unit. Int J Control Energy Electr Eng (CEE) 2019;8:1–6.

[35] Lv X, Lv Y, Zhu Y. Multi-variable study and MOPSO-based multi-objective optimization of a novel cogeneration plant using biomass fuel and geothermal energy: A complementary hybrid design. Energy 2023;270:126921.

[36] Kotas TJ. The Exergy Method of Thermal Plant Aanalysis. Paragon Publishing; 2012.

[37] Ion DOSA, Codrut PD. Efficiency assessment of condensing steam turbine. Adv Environ Ecosyst Sustain Tour 2013:203–8.

[38] Karakurt AS. Performance analysis of a steam turbine power plant at part load conditions. J Therm Eng 2017;3(2):1121–8.

[39] Moran MJ, Shapiro HN, Boettner DD, Bailey MB. Fundamentals of engineering thermodynamics. John Wiley & Sons; 2010.

[40] Prins MJ, Ptasinski KJ, Janssen FJ. From coal to biomass gasification: Comparison of thermodynamic efficiency. Energy 2007;32(7):1248–59.

[41] ANEO (Asociación Nacional de Empresas de Aceite de Orujo), *Biomasa.* https://www.aneorujo.es/biomasa/#orujillo. (accessed on June 2022).

[42] Sartor K, Restivo Y, Ngendakumana P, Dewallef P. Prediction of SOx and NOx emissions from a medium size biomass boiler. Biomass Bioenergy 2014;65:91–100.

[43] U.s.. Department of Energy. Check Burner Air to Fuel Ratios. Energy Tips-Process Heating 2007.

[44] F -Chart Software, *EES Engineering Equation Software*. https://www.fchartsoftware.com/ees/. [Accessed June 2023).

[45] Patiño-Duque HD, Rosero-Coral BD. Análisis exergético de una planta de cogeneración operando bajo ciclo combinado. Ingeniería Investigación y Desarrollo 2017;17(1):49–58.

[46] Imran KM. Irreversibility Analysis of Double Effect LiBr-Water Vapor Absorption Chiller. J Eng Sci Technol Rev 2013;6(5):115–22.

[47] Poljak I, Orović J, Mrzljak V. Energy and exergy analysis of the condensate pump during internal leakage from the marine steam propulsion system. Pomorstvo 2018;32(2):268–80.

[48] Navantia, *Intelligent and sustainable products and services*. https://www.navantia.es/en/. (Accessed June 2023).